Smart Structures and Systems, Vol. 10, No. 2 (2012) 155-179

DOI: http://dx.doi.org/10.12989/sss.2012.10.2.155

Evaluation and analytical approximation of Tuned Mass Damper performance in an earthquake environment

Alexander Tributsch and Christoph Adam*

Unit of Applied Mechanics, University of Innsbruck, Technikerstr. 13, 6020 Innsbruck, Austria

(Received September 27, 2011, Revised April 3, 2012, Accepted June 25, 2012)

Abstract. This paper aims at assessing the seismic performance of Tuned Mass Dampers (TMDs) based on sets of recorded ground motions. For the simplest configuration of a structure-TMD assembly, in a comprehensive study characteristic response quantities are derived and statistically evaluated. Optimal tuning of TMD parameters is discussed and evaluated. The response reduction by application of a TMD is quantified depending on the structural period, inherent damping of the stand-alone structure, and ratio of TMD mass to structural mass. The effect of detuning on the stroke of the TMD and on the structural response is assessed and quantified. It is verified that a TMD damping coefficient larger than the optimal one reduces the peak deflection of the TMD spring significantly, whereas the response reduction of the main structure remains almost unaffected. Analytical relations for quantifying the effect of a TMD are derived and subsequently evaluated. These relations allow the engineer in practice a fast and yet accurate assessment of the TMD performance.

Keywords: analytical reduction coefficients; detuning; multivariate regression analysis; optimal tuning; recorded ground motions; statistical response evaluation

1. Introduction

Improved and novel high-strength materials, advanced construction technologies, and refined methods of analysis allow the design of extremely slender structures, which exhibit in general rather light inherent damping. Consequently, many of these novel structures would be vibration prone, if no additional external or internal damping mechanisms are provided.

Installation of Tuned Mass Dampers (TMDs) is an effective measure to add damping to the structure. A TMD is a simple single-degree-of-freedom (SDOF) oscillator of either mass-spring-dashpot type, or a pendulum-dashpot system. If the natural frequencies of both substructures are accurately tuned, the kinetic energy is transferred from the structure to the TMD, where it is subsequently dissipated through the viscous damping element. The superiority of TMDs to mitigate narrow-band periodic vibrations induced by wind and traffic loads as well as rotating machines is well-established in the engineering community, whereas their performance to protect a structure against earthquake induced vibrations is still controversially discussed. For example, Casciati and Giuliano (2009) report about weak seismic performance of TMDs with very small mass ratios. In contrast,

*Corresponding author, Professor, E-mail: christoph.adam@uibk.ac.at

other papers (e.g., Adam and Furtmüller 2010) claim the efficiency of TMDs to mitigate seismic induced vibrations. Alternatively, semi-active TMDs have shown to reduce vibrations even more effectively (Woo 2011), but they rely on external power supply or battery power (Jagadish 2008). Passive TMD devices have proven to operate robustly in harsh environmental conditions without depending on any power supply. As outlined by Giuliano (2012) research on the behavior of TMDs under earthquakes is of continuing importance.

However, even if a TMD is designed to protect a building only against periodic vibration from e.g. wind, the design engineer is obliged to assess also the seismic TMD performance and its effect on the structure, if the building is located in an earthquake environment. For example, it must be ensured that the stroke of the TMD does not exceed a certain design limit when subjected to strong motion seismic excitation with low probability of occurrence (Wang *et al.* 2009, Meinhardt 2010). Exemplary, Wang *et al.* (2009) present a two-stage optimum design procedure for TMD considering limitation of the TMD stroke, because simultaneous minimization both of the structural and TMD response is not possible. The assessment of the seismic TMD performance may be a challenge, because information on the probability of exceedance of certain structural and non-structural response parameters requires in general computationally expensive time history analyses based on a several recorded ground motions and subsequent statistical evaluation of the derived response data.

The presented fundamental study aims at quantifying the seismic performance of TMDs. Preliminary results of this study have been presented in Tributsch *et al.* (2011). The simplest configuration of a structure with attached TMD is considered. Both, the structure and the TMD are modeled as SDOF systems of mass-spring-dashpot type, and they are connected in series. The inherent record-to-record variability of earthquake excitation is taken into account utilizing three different sets of recorded ground motions, which contain 44, 28 and 40 records, respectively. For a comprehensive range of characteristic structural parameters non-dimensional statistical response quantities such as median, 16% and 84% quantiles are derived. Nonlinear regression analyses are conducted to the derived data base of response quantities delivering design formulas for estimating the response of structure and TMD both efficiently and yet accurate for the early design phase.

2. Methodology

2.1 Mechanical model

A linear elastic vibration prone structure, whose fundamental mode dominates its dynamic response, may be represented as a one-story shear frame structure equipped with a dashpot damper. From mass m_1 of the rigid beam, story stiffness k_1, and viscous damping parameter r_1 its characteristic dynamic parameters, i.e., the natural circular frequency $\omega_1 = \sqrt{k_1/m_1}$ and the non-dimensional damping coefficient $\zeta_1 = r_1/(2\omega_1 m_1)$, are derived. The base acceleration $\ddot{x}_g$ induces structural vibrations expressed by the relative horizontal displacement x_1 of the beam with respect to the base.

A mass-spring-dashpot system of mass m_2, stiffness k_2, and damping parameter r_2 represents the TMD with a single dynamic degree-of-freedom. Its natural circular frequency $\omega_2 = \sqrt{k_2/m_2}$ and its damping coefficient $\zeta_2 = r_2/(2\omega_2 m_2)$ must be tuned appropriately to the corresponding quantities of the main structure, as discussed subsequently. The horizontal displacement x_2 (measured against the base) characterizes the motion of the TMD. Structure and TMD are connected in series, and thus represent a non-classically damped two-degrees-of-freedom (2DOF) system shown in Fig. 1.

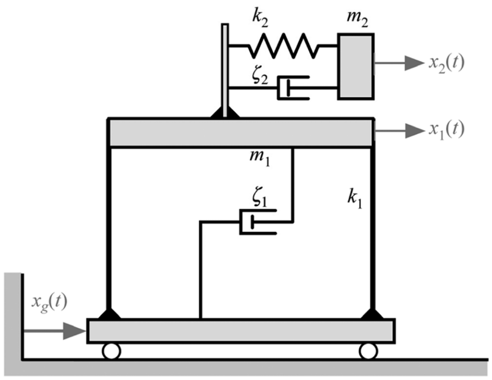

Fig. 1 Mechanical model of a simple structure equipped with a TMD and subjected to seismic excitation

2.2 Seismic excitation

The mechanical model is subjected to the time dependent base acceleration $\ddot{x}_g(t)$ from ground motions recorded during real earthquakes. In the FEMA P-695 (2009) report ("ATC 63 project") earthquake records with similar properties are classified into two sets, one containing far-field records, and the other near-field records. All ground motions of this report have been recorded on NEHRP Site Class B (rock), C (soft rock/very dense soil), or D (stiff soil) during earthquakes of magnitudes ≥6.5 (FEMA P-695 2009). The distance to fault rupture is less than 10 km for near-field records, and larger than or equal to 10 km for the far-field records.

28 of 56 records of the near-field set exhibit strong pulse characteristics. In the following the effect of ground motion pulses on the TMD performance is studied, and hence only those 28 records (denoted as ATC63-NFwP) are utilized after rotation in fault normal direction. The far-field set of 44 records is referred to as ATC63-FF set.

Furthermore, simulations based on a third set of ground motions, i.e., the LMSR-N bin, have been performed in an effort to confirm the findings of this study and to show their generality. This set of ordinary ground motion records contains 40 ground motions recorded in Californian earthquakes of moment magnitude between 6.5 and 7 and closest distance to the fault rupture between 13 km and 40 km on NEHRP site class D according to FEMA 368, 2000 (Medina and Krawinkler 2003).

It is of interest to evaluate the efficiency of the TMD in the phase of forced vibrations T_F plus a pre-defined time period T_D of subsequent decay of free vibrations. The selection of T_D is discussed later.

2.3 Dynamic response

Transformation of the acceleration record $\ddot{x}_g(t)$ into the frequency domain $\ddot{X}_g(\alpha)$, and subsequent multiplication with the complex frequency response function of the main structure $H_1(\alpha)$ and of the TMD $H_2(\alpha)$, renders the response of the structure and of the TMD $X_1(\alpha)$ and $X_2(\alpha)$, respectively, in the frequency domain

$$X_1(\alpha) = H_1(\alpha)\ddot{X}_g(\alpha), \quad X_2(\alpha) = H_2(\alpha)\ddot{X}_g(\alpha) \tag{1}$$

at which

$$H_1(\alpha) = \frac{1}{\omega_1^2} \frac{1+\mu Z(\alpha)}{(1-\alpha^2+2j\zeta_1\alpha)-\mu\alpha^2 Z(\alpha)}, \quad H_2(\alpha) = \frac{1}{\omega_1^2} \frac{1+\mu Z(\alpha)+Y(\alpha)}{(1-\alpha^2+2j\zeta_1\alpha)-\mu\alpha^2 Z(\alpha)} \tag{2}$$

and

$$Z(\alpha) = \frac{\beta^2+2j\zeta_2\alpha\beta}{\beta^2-\alpha^2+2j\zeta_2\alpha\beta}, \quad Y(\alpha) = \frac{1+2j\zeta_1\alpha}{\beta^2-\alpha^2+2j\zeta_2\alpha\beta} \tag{3}$$

α is defined as the ratio of the excitation frequency ν to the natural frequency ω_1 of the structure without TMD: $\alpha = \nu/\omega_1$. $\beta = \omega_2/\omega_1$ denotes the ratio of TMD to structural natural frequency, and μ is the mass ratio: $\mu = m_2/m_1$. The imaginary unit is denoted by j. Application of Inverse Fourier Transform to $X_1(\alpha)$ and $X_2(\alpha)$ yields the displacement of the main structure $x_1(t)$ and of the TMD $x_2(t)$ in the time domain.

2.4 Variation of parameters

Inspection of Eqs. (1) to (3) reveals that for given base acceleration $\ddot{x}_g$ the response of the coupled system depends on the following parameters: natural frequency ratio β, mass ratio μ, natural frequency ω_1 (or expressed alternatively by the period $T_1=2\pi/\omega_1$) of the stand-alone structure, and damping coefficients ζ_1 and ζ_2. For given mass ratio μ, period T_1 and damping coefficient ζ_1 of the structure, the parameters of the TMD, i.e., the frequency ratio β and TMD damping coefficient ζ_2, are optimized for optimal performance of the TMD. Usually, optimal performance of the TMD means that the response reduction is maximal. However, several other optimization criteria can be defined (Wang *et al.* 2009, Lee *et al.* 2006, Marano *et al.* 2010).

In this study, the responses for comprehensive combinations of these parameters (without optimization) were computed in a specified range, and stored in a database. Subsequently, the database was scanned for maximal reduced response quantities, and the corresponding optimal TMD parameters were compared with outcomes from different analytical and numerical optimization criteria. The utilized range of parameters is presented in Table 1. Note that mass ratios smaller than 2% are not relevant for the mitigation of earthquake-induced response. However, if the TMD is applied to reduce wind-induced vibrations a mass ratio of 0.5% might be effective. In such a case the seismic response of the TMD must be assessed, hence, the lower bound of the mass ratio of 0.5% was selected for this study. The largest considered mass ratio is 8%.

Table 1 Range of utilized structural parameters

	Parameter	Minimum	Maximum	Increment
T_1	period of the SDOF stand-alone structure	0.05 s	5.00 s	0.05 s
μ	ratio of TMD mass to structural mass	0.005	0.08	0.005
β	frequency ratio of TMD to stand-alone main structure	0.85	1.04	0.01
ζ_2	damping coefficient of the TMD	0.04	0.20	0.01
ζ_1	inherent damping of the stand-alone main structure	0.005, 0.01, 0.02, 0.03, and 0.05		

3. Characteristic response quantities

In this study the efficiency of a TMD is quantified through two different response reduction coefficients and one coefficient quantifying the stroke of the TMD. A response reduction coefficient represents the ratio of a specific response quantity of the main structure *with* attached TMD to the corresponding response quantity of the main structure *without* TMD. Thus, for linear structural behavior no scaling of earthquake records is required. Statistical evaluation of the individual reduction coefficients of each record set renders median, 16% and 84% quantiles, which are common values to characterize record-to-record variability in the seismic response.

3.1 Root-mean-square displacement reduction coefficient

A meaningful response quantity for assessing the TMD performance is the root-mean-square (RMS) of the structural displacement $x_1(t)$ with respect to time t. For the ith ground motion record of a record set the corresponding RMS reduction coefficient is defined as

$$R_i = \sqrt{\frac{\int_{(T_F+T_D)} x_{1,i}^2\Big|_{\text{with } TMD} dt}{\int_{(T_F+T_D)} x_{1,i}^2\Big|_{\text{no } TMD} dt}} \tag{4}$$

A reduction coefficient of zero indicates complete vibration absorption, whereas the TMD is non-effective for a value of one. If R_i is larger than one, the TMD impairs the performance of the main structure.

Statistically evaluated RMS displacement reduction coefficients for each ground motion set such as median, 16% and 84% quantiles are denoted as $R^{(med)}$, $R^{(16)}$, and $R^{(84)}$, respectively.

Integration with respect to time t includes forced vibrations and subsequent free vibrations. The free vibration response is considered up to the instant of time, where the estimated vibration amplitude $x_{1,n}$ is 20% of the initial amplitude $x_{1,0}$ at the end of the forced vibration phase T_F. This period denoted by T_D is assumed to be a multiple n of the structural period T_1

$$T_D \approx nT_1 \tag{5}$$

Starting point of estimating the time period T_D is the logarithmic damping decrement Λ of a fictitious SDOF oscillator with damping coefficient ζ_{ef} (Chopra 2007)

$$\Lambda = \frac{1}{n}\ln\left(\frac{x_0}{x_n}\right) \equiv 2\pi\zeta_{ef} \tag{6}$$

Thereby, x_0 is the initial vibration amplitude of free vibrations of the SDOF oscillator, and x_n denotes the amplitude n periods later. Eq. (6) is solved for the number of periods n. Replacing the vibration amplitudes of the fictitious SDOF system by the amplitudes $x_{1,0}$ and $x_{1,n}$ of the actual main structure (equipped with a TMD), and assuming that at $t = T_D$ the vibration amplitude of the main structure is 20% of the initial one, $x_{1,n} = 0.2x_{1,0}$, one obtains

$$n = \frac{1}{2\pi\zeta_{ef}}\ln\left(\frac{x_0}{x_n}\right) = \frac{1}{2\pi\zeta_{ef}}\ln\left(\frac{x_{1,0}}{0.2x_{1,0}}\right) \approx \frac{1.6}{2\pi\zeta_{ef}} \tag{7}$$

The damping coefficient ζ_{ef} can be estimated from the peak dynamic magnification factor $\max V(\alpha)$ of the fictitious SDOF system

$$\zeta_{ef} = \frac{1}{2\max V(\alpha)} \tag{8}$$

However, $\max V(\alpha)$ is replaced by the dynamic peak magnification $\max V_1(\alpha)$ of an undamped SDOF main system equipped with an optimally tuned TMD assuming *harmonic* base acceleration and minimization of the structural displacement, see Warburton (1982)

$$\max V_1(\alpha) = (1+\mu)\sqrt{\frac{2}{\mu}} \tag{9}$$

This expression is utilized, because for random base acceleration $V_1(\alpha)$ is defined as a RMS displacement instead of a maximum displacement (Warburton 1982). Introducing Eq. (9) into Eq. (8), Eq. (8) into Eq. (7), and Eq. (7) into Eq. (5) leads to the length of time of the free vibrations considered in the response evaluation

$$T_D \approx 1.6 T_1 \frac{1+\mu}{\pi}\sqrt{\frac{2}{\mu}} \tag{10}$$

3.2 Peak displacement reduction coefficient

Another characteristic response quantity is the peak displacement of the main structure. For seismic excited structures this quantity is often most significant because it can be directly related to structural damage (Giuliano 2012). Relating the peak displacement of the structure equipped with TMD to this response quantity of the stand-alone structure yields the peak displacement reduction coefficient related to the ith ground motion

$$P_i = \frac{\max|x_{1,i}|_{\text{with TMD}}}{\max|x_{1,i}|_{\text{no TMD}}} \tag{11}$$

Statistical evaluation of the individual peak displacement reduction coefficients leads for each ground motion set separately median $P^{(med)}$, 16% quantile $P^{(16)}$, and 84% quantile $P^{(84)}$.

3.3 TMD stroke coefficient

The stroke of the TMD (i.e. TMD peak displacement with respect to its attachment point at the main structure) is an important design parameter to assure the efficiency of the TMD, and to avoid damage of the TMD and/or of the main structure. In the present study this quantity is related to the corresponding peak displacement of the main structure without TMD, and thus leading to the TMD stroke coefficient

$$D_i = \frac{\max|x_{2,i} - x_{1,i}|_{\text{with TMD}}}{\max|x_{1,i}|_{\text{no TMD}}} \tag{12}$$

Median, 16% quantile, and 84% quantile for all stroke coefficients of one record set are denoted by $D^{(med)}$, $D^{(16)}$, and $D^{(84)}$, respectively.

4. Optimal TMD parameters

4.1 Mass ratio

Additionally to the natural frequency ratio β and the damping coefficient ζ_2, also mass ratio μ may be considered as a TMD parameter. In general, a larger μ results in smaller reduction coefficients, i.e., in a better performance of the TMD. Since a TMD increases the total mass of the system, a reasonable mass ratio for a single TMD is between about 2% and 8%. In this study, the mass ratio is considered as a design parameter selected in advance, whereas parameters β and ζ_2 must be tuned optimally.

4.2 Optimal natural frequency ratio

The kinetic energy is transferred from the structure to the TMD, and subsequently dissipated in the dashpot damper of the TMD. This energy transfer is most effective, if the TMD is in resonance with the main structure. Thus, the natural frequency of the TMD should be closely spaced to the natural frequency of the main structure, i.e. the optimal natural frequency ratio β_{opt} is close to one.

Warburton (1982) derived analytical expressions for optimal parameters of a TMD attached to an undamped SDOF main structure ($\zeta_1 = 0$) subjected to white noise base acceleration. Minimizing the RMS of the main structure displacement leads to the following optimal frequency ratio (Warburton 1982)

$$\beta_{opt} = \frac{\sqrt{1-\mu/2}}{1+\mu} \tag{13}$$

which is a function of the mass ratio μ only. To account for viscous damping of the main structure, $\zeta_1 \neq 0$, Hoang *et al.* (2008) propose to modify this optimal frequency ratio according to

$$\beta_{opt}^{(\zeta_1 \neq 0)} = \beta_{opt} - \frac{0.7\zeta_1}{1-\mu/2} \tag{14}$$

In the present study decreasing β_{opt} by about $\zeta_1/2$ was found to yield the best, however only insignificantly improved, TMD performance in the considered parameter range. Certainly, for each ground motion record or set of ground motions and for each combination of μ, T_1, and ζ_1 an optimal frequency ratio β may be determined. However, small variations of these design parameters would lead to quite a large and irregular scatter of the optimal frequency ratio β. The achievable improvement of the median seismic TMD performance by application of individual (for future events in advance unpredictable) optimal frequency ratios would typically be smaller than 5%, compared to the outcomes based on the optimal frequency ratio of Eq. (13).

For white noise excitation β_{opt} does not depend on the structural period T_1, because the energy is uniformly distributed in the frequency domain. However, when the system is subjected to recorded ground motions, the optimal frequency ratio β becomes period dependent. Marano *et al.* (2007) showed that this effect can be observed also for Kanai-Tajimi filtered white noise base acceleration. Results of the present study based on the ATC63 ground motion sets suggest that for short period systems ($T_1 \leq 0.20$s) β_{opt}, Eq. (13), should be reduced by 0.02 to give minimum response reduction coefficients. In contrast, for long period systems with $T_1 = 5.0$s optimal TMD performance is achieved for β_{opt}, Eq. (13), increased by 0.02. This small change in β_{opt} reduces that peak (out of two) of the frequency response function $H_1(\alpha)$, where the corresponding frequency content of the earthquake record is larger. The simultaneous increase of the second peak of $H_1(\alpha)$ has a small effect on the response, because of lower excitation energy at the corresponding frequencies.

From the outcomes of this study it can be concluded that tuning of the frequency ratio according to Eq. (13) is sufficient, because the improvements of the TMD efficiency by individual tuning is rather negligible and even not possible for future events.

4.3 Optimal TMD damping coefficient

For white noise excitation of an undamped main structure the following analytical expression for optimal TMD damping has been derived (Warburton 1982)

$$\zeta_{2,opt} = \sqrt{\frac{\mu(1-\mu/4)}{4(1+\mu)(1-\mu/2)}} \tag{15}$$

This expression can be utilized also for slightly damped main structures (i.e., $\zeta_1 \neq 0$). The invariance of $\zeta_{2,opt}$ with respect to variation of ζ_1 is shown in Ankireddi and Yang (1996) and Rüdinger (2006), and has also been observed in the present study based on recorded ground motions. Hoang *et al.* (2008) suggest a modified relation for optimal TMD damping, resulting in maximum changes of 0.001 for $\zeta_{2,opt}$, Eq. (15), within the parameter range considered here. Furthermore, this study has shown a negligible dependence of $\zeta_{2,opt}$ on the period T_1.

Thus, tuning of the TMD damping coefficient according to Eq. (15) leads to satisfactory TMD performance.

5. Parametric study

In the following, selected results of the parametric study, which characterize the seismic performance of TMDs, are presented.

5.1 Median response reduction coefficients

At first, the effect of a TMD on the earthquake induced median response of the main structure is evaluated. Thereby, the median response is characterized by the median RMS displacement reduction coefficient $R^{(med)}$ and median peak displacement reduction coefficient $P^{(med)}$. In Figs. 2 and 3 contour plots of $R^{(med)}$ and $P^{(med)}$, respectively, are shown as a function of the structural period T_1 and mass ratio μ. A period range of $0.05\ \text{s} \leq T_1 \leq 5.0\ \text{s}$ is considered, i.e., the study covers a wide range of stiff to flexible structures. The range of mass ratios, $0.02 \leq \mu \leq 0.08$, correlates to mass ratios of TMDs applied in practice. The presented results are based on TMD parameters β_{opt} and $\zeta_{2,opt}$ optimized according to Eqs. (13) and (15), respectively. Inherent damping ζ_1 of 1% (Figs. 2(a) and 3(a)), 3% (Figs. 2(b) and 3(b)), and 5% (Figs. 2(c) and 3(c)) is assigned to the main structure. The outcomes presented in these figures are based on the far-field ground motion set ATC63-FF.

The contour plot of $R^{(med)}$ shown in Fig. 2(a) demonstrates that this response reduction quantity is for all combinations of T_1 and μ smaller than one. A reduction of 40% to 55% can be observed compared to the structural response without attached TMD, i.e., $R^{(med)}$ is between 0.60 and 0.45.

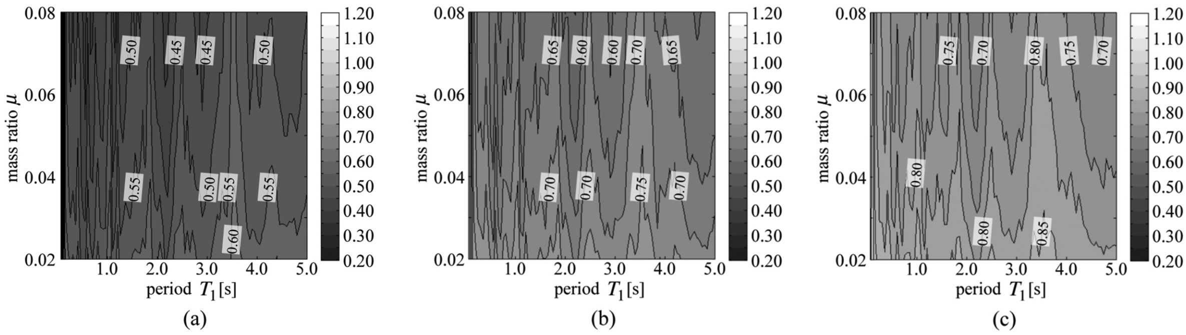

Fig. 2 RMS displacement reduction coefficient. Median. Far-field ground motion set. (a) $\zeta_1 = 0.01$, (b) $\zeta_1 = 0.03$ and (c) $\zeta_1 = 0.05$. β_{opt} and $\zeta_{2,opt}$ (Parameters see Table 1)

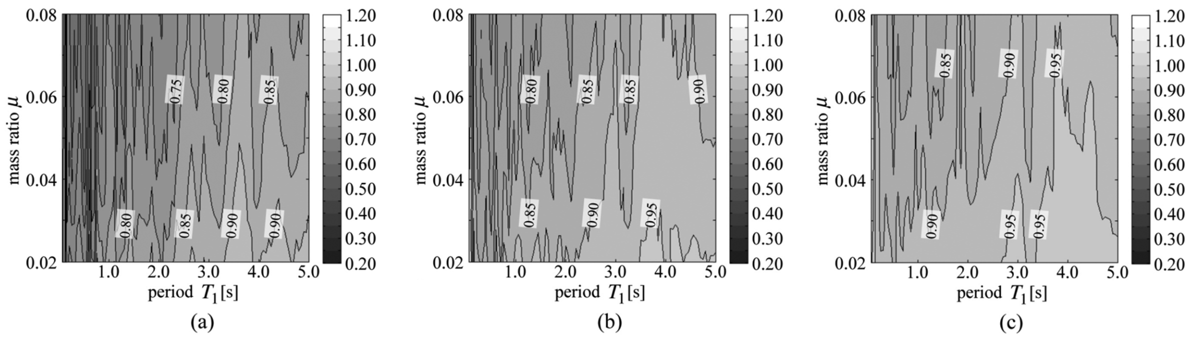

Fig. 3 Peak displacement reduction coefficient. Median. Far-field ground motion set. (a) $\zeta_1 = 0.01$, (b) $\zeta_1 = 0.03$ and (c) $\zeta_1 = 0.05$. β_{opt} and $\zeta_{2,opt}$ (Parameters see Table 1)

Note that $\zeta_1 = 0.01$. Furthermore, it is readily observed that, as expected, the performance of the TMD increases with increasing mass ratio μ. However, the improvement from mass ratio $\mu = 0.02$ to mass ratio $\mu = 0.08$ is on average 15 percentage points only. For very stiff systems ($T_1 \leq 0.10$ s) the TMD efficiency is poor. In the acceleration sensitive medium period range between 0.2 and 1.5 s the TMD performance is superior.

When structures possess larger inherent damping of the stand-alone structure, i.e., they are less vibration prone, TMDs are less efficient to mitigate the earthquake induced response. This conclusion is confirmed by the results of Figs. 2(b) and (c), where the reduction coefficient $R^{(med)}$ is depicted for $\zeta_1 = 0.03$ and 0.05, respectively. $R^{(med)}$ is between 0.70 and 0.85 for $\zeta_1 = 0.05$, depending on the mass ratio and the period, see Fig. 2(c). For example, a structure-TMD assembly with $T_1 = 2.0$ s and $\mu = 0.05$ exhibits a reduction factor of $R^{(med)} = 0.45$, if $\zeta_1 = 0.01$, whereas for $\zeta_1 = 0.05$ the reduction coefficient is $R^{(med)} = 0.75$ only, compare Fig. 2(a) with 2(c). A TMD even impairs the structural response behavior for very stiff systems.

For inherent damping of the stand-alone structure of $\zeta_1 = 0.01$ application of a TMD yields a reduction of the median peak displacement response $P^{(med)}$ between 10% and 30%, i.e., $P^{(med)}$ is between 0.90 and 0.70, see Fig. 3(a). However, if $\zeta_1 = 0.05$, the reduction of the median peak response is at most 15%, and almost negligible for small mass ratios, compare Fig. 3(c).

Additionally, Fig. 4 shows for discrete mass ratios μ of 0.02, 0.04, 0.06, and 0.08 reduction

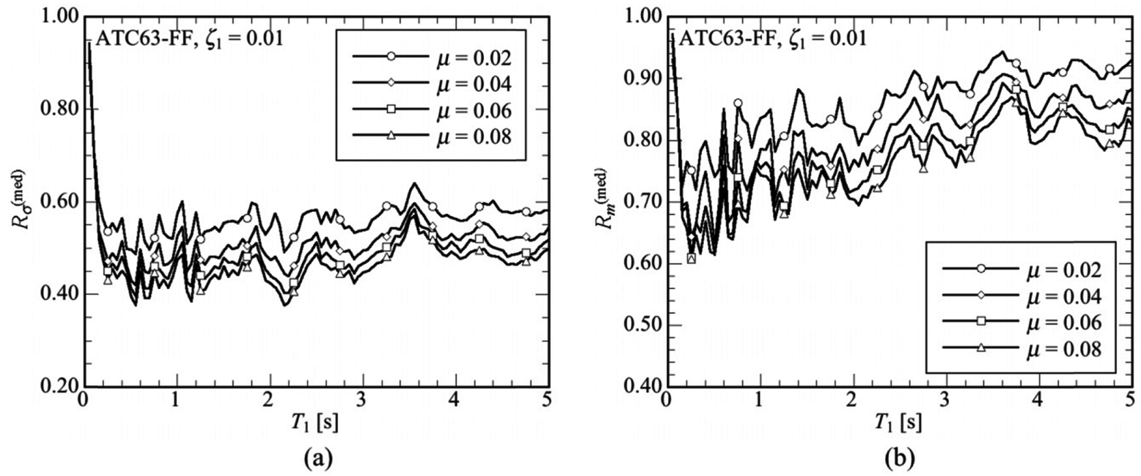

Fig. 4 (a) RMS displacement reduction coefficient and (b) peak displacement reduction coefficient. Median. Far-field ground motion set. $\zeta_1 = 0.01$. β_{opt} and $\zeta_{2,opt}$

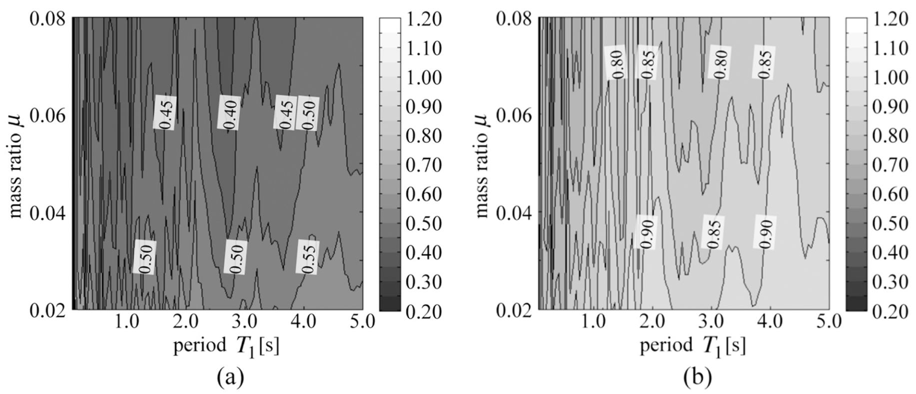

Fig. 5 (a) RMS displacement reduction coefficient and (b) peak displacement reduction coefficient. Median. Near-field ground motion with pulse set. $\zeta_1 = 0.01$. β_{opt} and $\zeta_{2,opt}$

coefficients $R^{(med)}$ and $P^{(med)}$, respectively, plotted against the structural period T_1. Low inherent damping of the main structure of $\zeta_1 = 0.01$ is examined. With increasing mass ratio the performance of the TMD is enhanced. For very stiff structures the effect of the TMD to reduce vibrations is poor. However, in the acceleration sensitive period range $0.2\ \text{s} \le T_1 \le 1.5\ \text{s}$ the efficiency of the TMD is superior, and afterwards decreases continuously with increasing period T_1.

Subsequently, median reduction coefficients $R^{(med)}$ and $P^{(med)}$ based on the near-field ground motion set ATC63-NFwP are discussed. In Fig. 5 contour plots of these quantities are presented for structures exhibiting inherent damping of $\zeta_1 = 0.01$. Comparison of Fig. 5(a) with Fig. 2(a) reveals that a TMD reduces the structural RMS displacement response induced by near-field ground motions more effectively. However, as shown later, the difference between near-field and far-field RMS displacement response is statistically negligible. In contrast, from Figs. 5(b) and 3(a) it is observed that the median peak response $P^{(med)}$ is mitigated more effectively for excitation by the far-field set.

This contradictory behavior can be attributed to the fact that ground motions containing pulses induce larger initial displacements when the TMD is nearly inactive, resulting in larger values of $P^{(med)}$ compared to the response induced by far-field records. In some cases the peak displacement of a structure with attached TMD even exceeds the response of the stand-alone structure. Most of the kinetic energy is transferred to the structure during the pulse, but subsequently the response can be mitigated almost undisturbed by an optimally tuned TMD, because the remaining energy input to the system is almost negligible. Thus, $R^{(med)}$ is in general smaller for excitation by the near-fault records with pulses, but statistically negligible as discussed below.

In a study based on analytical white noise (Schmelzer *et al.* 2010) the TMD performance expressed by reduction coefficients is similar except for very short periods. This difference can be attributed to the fact that the frequency content in most of the considered ground motion records is almost zero for frequencies larger than 10 to 20 Hz (the sampling rate is 50 to 200 Hz). If the natural frequency of the SDOF structure is larger than 10 Hz (i.e., $T_1 < 0.1$ s), the frequency response function is almost one (in non-dimensional form) for most frequencies contained in the ground motion records. Thus, attaching a TMD leads in the low frequency range to an amplification of the frequency response function $H(\alpha)$ of the SDOF structure by a factor of $(1+\mu)$, and subsequently, structural responses without and with TMD approach each other when the period T_1 is very small. A more detailed study of the response in the short period range revealed that a TMD with larger mass ratio can even impair the response for periods $T_1 \leq 0.10$ s. In contrast, analytical white noise contains the same amount of energy at each frequency (i.e., also at very low periods), and thus, this effect does not occur.

5.2 Dispersion of response reduction coefficients

Next, the dispersion of the individual reduction coefficients is assessed based on the 16% and 84% quantiles. Fig. 6 shows contour plots of $R^{(16)}$ and $R^{(84)}$ for $\zeta_1 = 0.01$ and the far-field ground motion set ATC63-FF. The general trend of these quantiles is the same as for the corresponding median. From Fig. 6(a) an $R^{(16)}$ between 0.50 and 0.30 can be identified, the 84% quantiles are between 0.85 and 0.60, see Fig. 6(b). The corresponding median of this quantity $R^{(med)}$ is between 0.60 and 0.45, compare Fig. 2(a).

The quantiles of the peak displacement reduction coefficients $P^{(16)}$ and $P^{(84)}$ are plotted in Fig. 7.

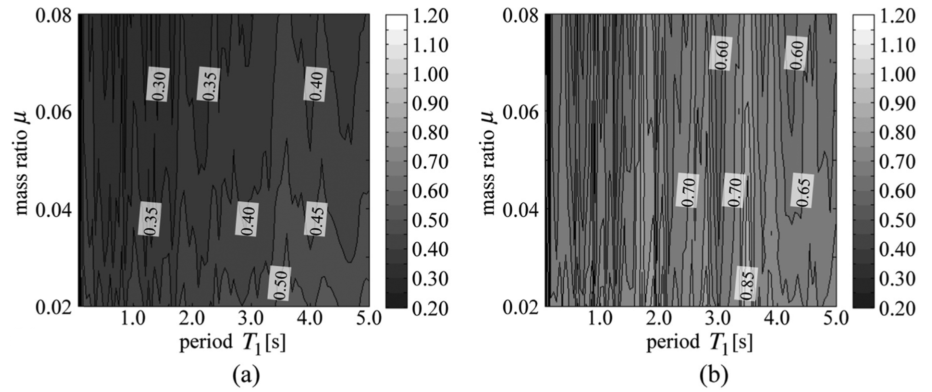

Fig. 6 RMS displacement reduction coefficient. (a) 16% quantile and (b) 84% quantile. Far-field ground motion set. $\zeta_1 = 0.01$. β_{opt} and $\zeta_{2,opt}$

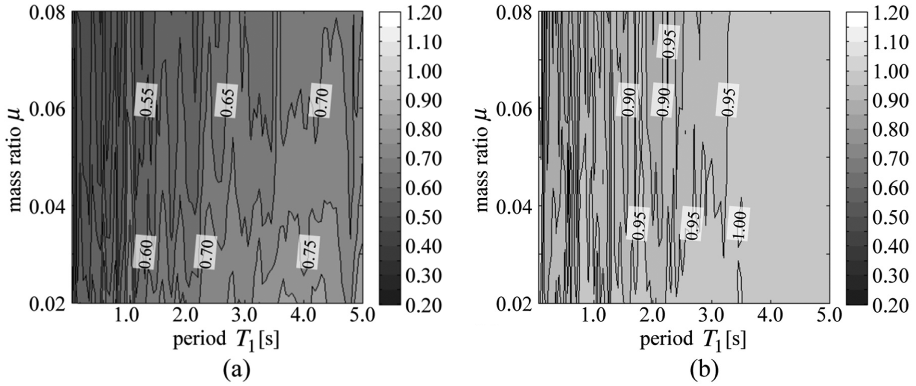

Fig. 7 Peak displacement reduction coefficient. (a) 16% quantile and (b) 84% quantile. Far-field ground motion set. $\zeta_1 = 0.01$. β_{opt} and $\zeta_{2,opt}$

It is interesting to observe that for flexible systems with periods T_1 larger than 3.5 s $P^{(84)}$ is close to one, i.e., for this statistical quantity the TMD has no effect on the structural peak displacement, see Fig. 7(b). For periods 0.15 s < T_1 < 3.5 s $P^{(84)}$ is slightly smaller than one.

For selected mass ratios μ of 0.02, 0.05, and 0.08, and for discrete structural periods T_1 in the range between 0.05 s and 5.0 s the dispersion of the individual peak displacement coefficients P_i is

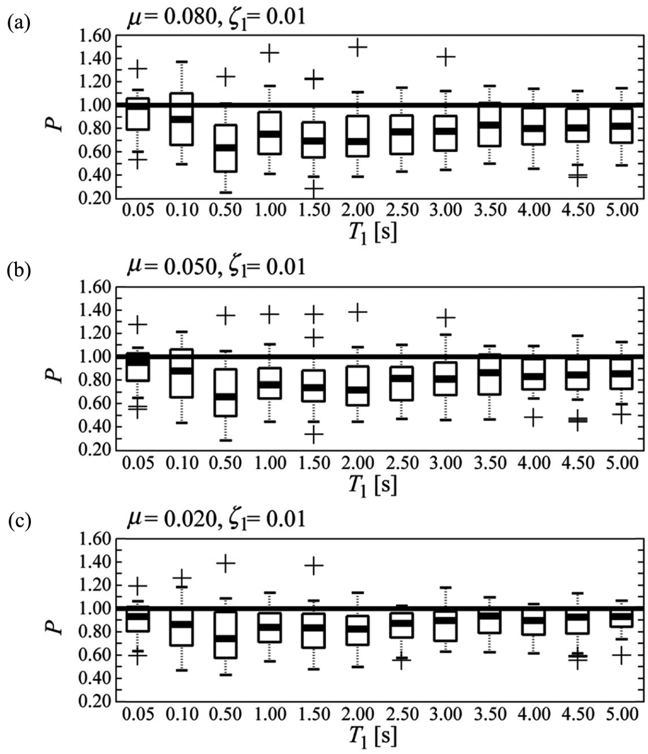

Fig. 8 Peak displacement reduction coefficient. Statistical evaluation - boxplots. (a) $\mu = 0.08$, (b) $\mu = 0.05$ and (c) $\mu = 0.02$. Far-field ground motion set. $\zeta_1 = 0.01$. β_{opt} and $\zeta_{2,opt}$

studied in more detail. ζ_1 is 1%, and the excitation is provided by the far-field ground motion set ATC63-FF, as before. Fig. 8 shows boxplots for P_i, however, in contrast to the common form the upper and lower lines of a box itself show 16% and 84% quantiles instead of 25% and 75% quantiles. The bold line inside a box symbolizes the median value, outliers are marked with a "+", and the upper and lower whiskers give minimum and maximum values, reassessed considering the outliers. Note, that the definition of the maximum whisker is usually based on the 25% and 75% quantiles (McGill *et al.* 1978). However, for this study the definition is adjusted for 16% and 84% quantiles assuming Gaussian distribution. The bold line at $P_i = 1$ separates the range of maximum displacement reduction ($P_i < 1$) from amplification ($P_i > 1$).

The median of P_i is smaller than one for all considered cases and in general between 0.70 and 0.90. All 84% quantiles except at $T_1 = 0.05$ s and $T_1 = 0.10$ s remain below the threshold of one. $P^{(84)}$ is close to one at $T_1 \geq 3.5$ s. i.e., a TMD leads in a statistical sense to a response reduction of earthquake excited structural vibrations. For all considered combinations of μ and T_1 at least one record can be found, which leads to a P_i larger than one. Attempts have been made to find parameters β and ζ_2 that minimize the maximum P_i within a ground motion set. In the considered range of parameters no solution has been found to guarantee reduction coefficients for maximum displacement below or close to one.

5.3 Median TMD stroke coefficient

Fig. 9 shows contour plots of the median values of the TMD stroke coefficient $D^{(med)}$ for ζ_1 of 1% (Fig. 9(a)), 3% (Fig. 9(b)), and 5% (Fig. 9(c)). It is observed that $D^{(med)}$ is reduced with increasing mass ratio. The effected of period T_1 and inherent damping of the stand-alone structure ζ_1 on this coefficient is small. For $\mu = 0.02$ coefficient $D^{(med)}$ is in average 3.25, for $\mu = 0.08$ $D^{(med)}$ is about 1.75.

5.4 Dispersion of the TMD stroke coefficient

The 16% and 84% quantiles $D^{(16)}$ and $D^{(84)}$, respectively, of the TMD stroke coefficient are depicted in Fig. 10. The results are based on inherent damping of $\zeta_1 = 0.01$, and optimal TMD parameters according to Eqs. (13) and (15). The 16% quantiles $D^{(16)}$ exhibit for small mass ratio $\mu = 0.02$ a value of 3.00, for large mass ratio $\mu = 0.08$ a value of 1.25, $D^{(84)} \approx 3.75$ for $\mu = 0.02$, and ≈ 2.00 for $\mu = 0.08$.

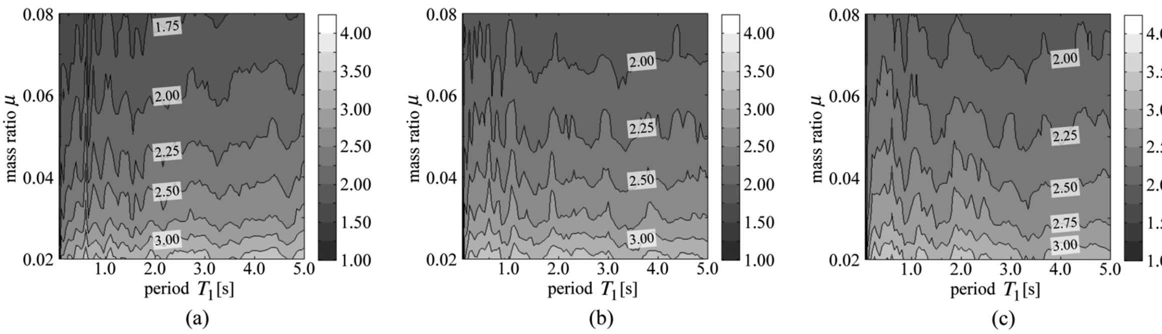

Fig. 9 TMD stroke coefficient. Median. Far-field ground motion set. (a) $\zeta_1 = 0.01$, (b) $\zeta_1 = 0.03$ and (c) $\zeta_1 = 0.05$. β_{opt} and $\zeta_{2,opt}$

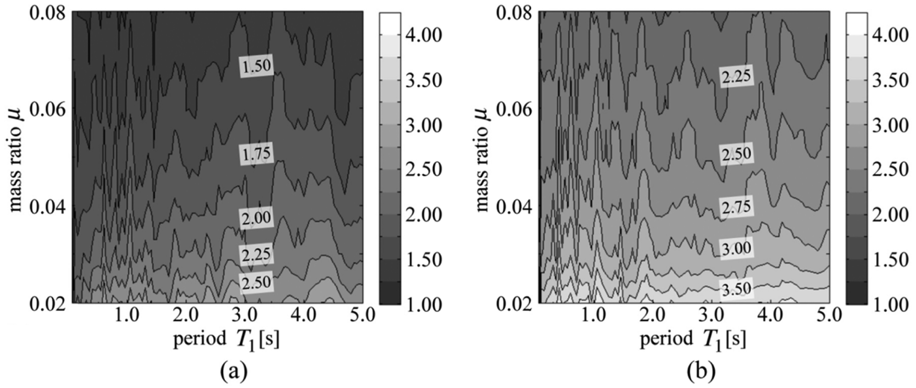

Fig. 10 TMD stroke coefficient. (a) 16% quantile and (b) 84% quantile. Far-field ground motion set. $\zeta_1 = 0.01$. β_{opt} and $\zeta_{2,opt}$

5.5 Effect of detuned TMD parameters

Next, the effect of intentional detuning of the TMD parameters from its optimal values is discussed in an effort to evaluate the robustness of the seismic TMD performance to uncertainty in its parameters. Systems subjected to the records of far-field set ATC63-FF with the following properties are considered: Viscous damping of the main structure $\zeta_1 = 0.01$, mass ratios μ of 0.02, 0.05, 0.08, and decoupled structural periods T_1 of 0.5 s, 1.0 s, 2.0 s and 4.0 s.

In Fig. 11 contour plots of median RMS displacement reduction coefficients $R^{(med)}$ are shown for

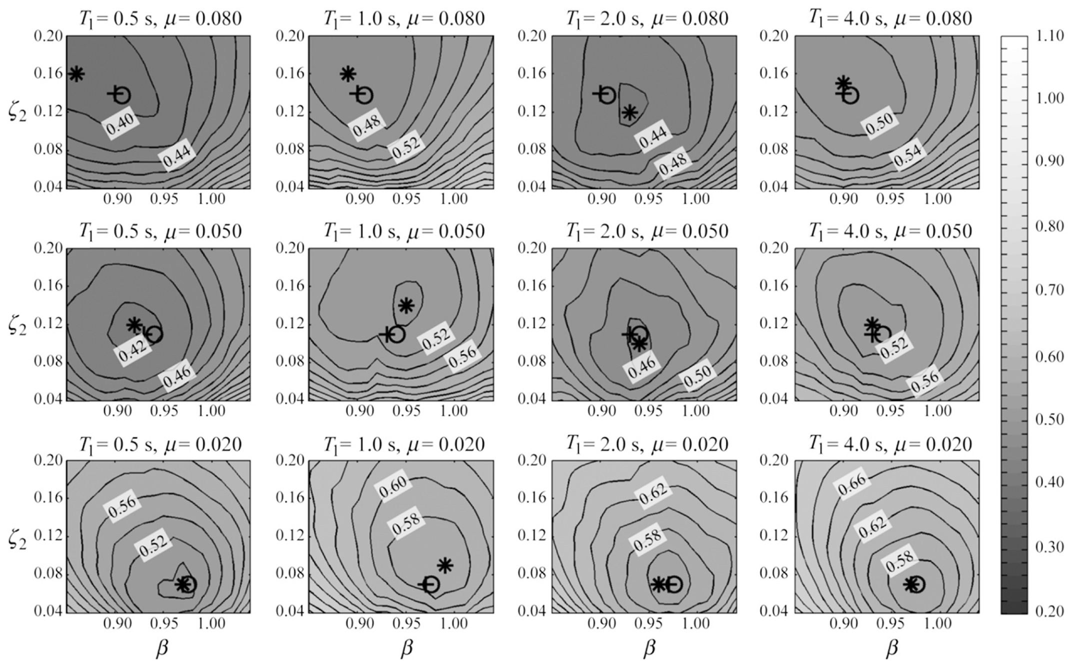

Fig. 11 RMS displacement reduction coefficient. Median. Far-field ground motion set. $\zeta_1 = 0.01$. Discrete pairs of T_1 and μ. Effect of detuned β and ζ_2 (Parameters see Table 1)

the TMD parameter ranges $0.04 \le \zeta_2 \le 0.20$ and $0.85 \le \beta \le 1.04$. In the individual figures several optimal values of β and ζ_2 are depicted: The assumption of white noise base acceleration and 1% inherent damping of the stand-alone structure leads to optimal parameters highlighted by "+". For these TMD parameters Lyapunov's equation was utilized to determine the minimum RMS of the displacement response, see e.g., Hoang *et al.* (2005). An "o" marks the analytically derived values β_{opt} and $\zeta_{2,opt}$ according to Eqs. (13) and (15), respectively, for white noise excitation and zero damping of the stand-alone structure. An asterisk indicates the actual minimum of $R^{(med)}$ identified by scanning the response data of the conducted parametric study.

Inspection reveals that for each configuration all optimal parameters are closely spaced. This outcome demonstrates that tuning according to Eqs. (13) and (15) is sufficient for earthquake excited structural vibrations.

Furthermore, it can be seen that the TMD performance is robust with respect to detuning of the TMD damping coefficient ζ_2. For this parameter the range $\zeta_2 = 0.12 \pm 66\%$ is depicted. However, detuning of the frequency ratio has a grave effect on the TMD efficiency. For this parameter only the frequency ratio range $\beta = 0.95 \pm 10\%$ is shown. A similar effect has been shown in Bachmann and Weber (1995) for harmonically excited systems.

For the same set of parameters the stroke coefficient $D^{(med)}$ is plotted in Fig. 12. Compared to the response of the main structure the behavior of this quantity is completely different with respect to detuning of β and ζ_2. It can be observed that increasing viscous damping from its optimal value to $\zeta_2 = 0.20$ reduces $D^{(med)}$ up to 50%. However, detuning with respect to the frequency ratio β in the depicted parameter range does not affect the relative displacement of the TMD considerably.

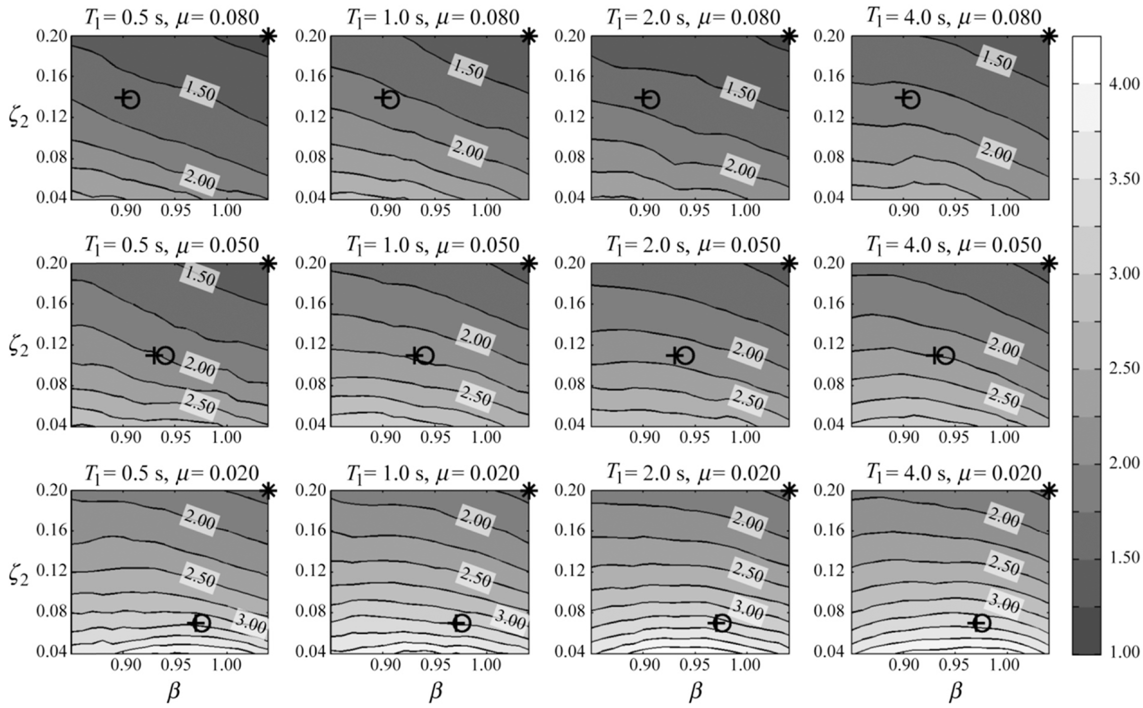

Fig. 12 TMD stroke coefficient. Median. Far-field ground motion set. $\zeta_1 = 0.01$. Discrete pairs of T_1 and μ. Effect of detuned β and ζ_2

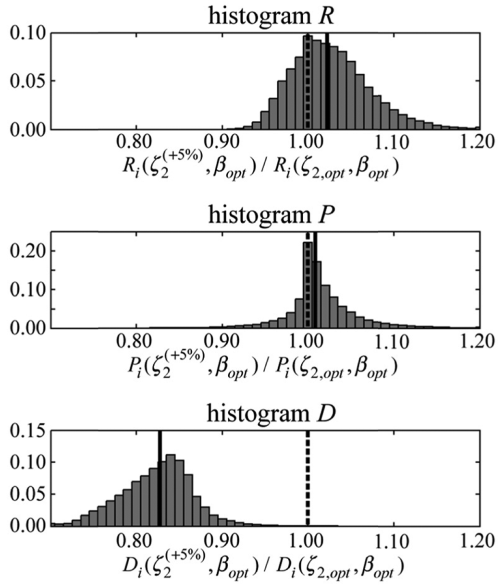

Fig. 13 Effect of detuned ζ_2. (a) RMS displacement reduction coefficient ratio, (b) peak displacement reduction coefficient ratio and (c) TMD stroke coefficient ratio. Evaluated for 57,200 combinations of 44 far-field records, varying T_1 and μ. $\zeta_1 = 0.01$. β_{opt}

Comparing the characteristics of the above discussed coefficients with respect to detuning of the TMD parameters leads to the well-known conclusion that a damping coefficient larger than its optimal value, $\zeta_2 > \zeta_{2,opt}$, improves the overall system behavior: $D^{(med)}$ is reduced considerably, whereas simultaneously the impairment of the structural response reduction capability of the TMD is negligible. This outcome is of importance, because in real applications the maximum spring deflection of the TMD is limited due to mechanical constraints.

Another representation of the effect of detuning is shown in Fig. 13. The histograms of this figure are based on the ratios of detuned response quantities to the corresponding tuned ones. Damping ζ_1 is 0.01. In particular, the optimal damping coefficient $\zeta_{2,opt}$ is increased by five percentage points to yield the detuned coefficient $\zeta_2^{(+5\%)}$. Subsequently, the counted number of response ratios per bin from all discrete combinations of period T_1 and mass ratio μ are plotted against the ratio bins (normalized to an area of one), leading to the histograms of Fig. 13. In particular, the results of the individual RMS displacement reduction coefficient ratios $R_i(\zeta_2^{(+5\%)}, \beta_{opt})/R_i(\zeta_{2,opt}, \beta_{opt})$ are presented in Fig. 13(a). Fig. 13(b) refers to the ratios P_i $(\zeta_2^{(+5\%)}, \beta_{opt})/P_i$ $(\zeta_{2,opt}, \beta_{opt})$, and the stroke ratios $D_i(\zeta_2^{(+5\%)}, \beta_{opt})/D_i(\zeta_{2,opt}, \beta_{opt})$ are depicted in Fig. 13(c). All results are derived from 57,200 individual combinations of T_1, μ and 44 earthquake records of the ATC63-FF ground motion set. A ratio of one means that the result based on tuned and detuned TMD damping is equal. Is the ratio smaller than one, the corresponding response coefficient based on detuned TMD damping is smaller than the corresponding one utilizing tuned TMD damping.

From Figs. 13(a) and (b) it can be seen that increasing of TMD damping with respect to its tuned counterpart may lead to an increase or to a decrease of the response reduction coefficient in a narrow band. The median of the reduction coefficients is increased slightly (about 1% to 2%) depending on the coefficient. On the other hand, the median of the TMD peak displacement coefficient ratio is decreased considerably by 17%. Consequently, the damping coefficient should be selected larger than the optimal one.

6. Analytical approximation of the response quantities

6.1 Basic equations

An outcome of the presented parametric study is a database of response quantities of the considered structure-TMD system, which covers a comprehensive range of parameters. In an effort to provide the engineer in practice with the essential results of this study, analytical relations for predicting the seismic response behavior of TMDs are derived based on non-linear multiple regression analysis. These analytical relations are valid for mass ratios in the range between 0.5% and 8%. They are simple to apply and yet sufficiently accurate to assess the seismic performance of a TMD in a practical design and evaluation process. Subsequently, the fundamentals of these equations are presented.

The analytical approximation of the reduction coefficients for optimal TMD parameters β_{opt} and $\zeta_{2,opt}$ according to Eqs. (13) and (15), respectively, is based on the following equation

$$\hat{R}^{(\psi)}(\zeta_{2,opt}, \beta_{opt}) = a^{(\psi)}T_1 + \frac{b^{(\psi)}}{T_1 + c^{(\psi)}} + d^{(\psi)}T_1\sqrt{\zeta_1} + e^{(\psi)}(0.05 - \zeta_1)(T_1 - f^{(\psi)})^2 + g^{(\psi)}\mu\zeta_1$$
$$+ \frac{h^{(\psi)}}{\mu + i^{(\psi)}}\left(1 - e^{-250(j^{(\psi)} - \zeta_1)}\right) + k^{(\psi)}\zeta_1^{l^{(\psi)}} + m^{(\psi)} \tag{16}$$

$$\hat{P}^{(\psi)}(\zeta_{2,opt}, \beta_{opt}) = \tilde{a}^{(\psi)}T_1\zeta_1 - (\tilde{b}^{(\psi)}T_1 - \tilde{c}^{(\psi)})^2(0.05 - \zeta_1) + \frac{\tilde{d}^{(\psi)}}{\mu + \tilde{e}^{(\psi)}}\left(1 - e^{-f^{(\psi)}\zeta_1 + \tilde{g}^{(\psi)}}\right)(1 - \tilde{h}^{(\psi)}T_1)$$
$$+ \tilde{i}^{(\psi)}\zeta_1 + \tilde{j}^{(\psi)} \tag{17}$$

The cap $\hat{}$ distinguishes the approximated reduction coefficient from the actual one of the database. Index ψ identifies the median, 16%, and 84% percentile of this displacement coefficient. E.g., if in Eq. (17) for ψ the quantity *med* is assigned, the median peak reduction coefficient $\hat{P}^{(med)}(\zeta_{2,opt}, \beta_{opt})$ is identified. Expressions (16) and (17) have been found in an iterative procedure to approximate the overall behavior of the reduction coefficients with respect to T_1, ζ_1, and μ. Coefficients $a^{(\psi)}$ to $m^{(\psi)}$, and $\tilde{a}^{(\psi)}$ to $\tilde{j}^{(\psi)}$ are determined through minimization of the relative error in the least-square sense between the analytical approximation and its counterpart from the parametric study. Selected coefficients are presented in Appendix A. The full set of coefficients is listed in Tributsch and Adam (2012).

For the stroke coefficient based on optimal TMD parameters β_{opt} and $\zeta_{2,opt}$ the corresponding analytical counterpart depends on T_1, ζ_1, and μ according to

$$\hat{D}^{(\psi)}(\zeta_{2,opt}, \beta_{opt}) = \bar{a}^{(\psi)}T_1 + \bar{b}^{(\psi)}\mu T_1 + \bar{c}^{(\psi)}\zeta_1 T_1 + \bar{d}^{(\psi)}\mu + \frac{\bar{e}^{(\psi)}}{\mu + \bar{f}^{(\psi)}\zeta_1^{\bar{g}^{(\psi)}}}\left(1 - e^{-\bar{h}^{(\psi)}T_1 + \bar{i}^{(\psi)}}\right)$$
$$+ j^{(\psi)}\zeta_1^{\bar{k}^{(\psi)}} + \bar{l}^{(\psi)} \tag{18}$$

Again, index ψ stands for the median, 16%, and 84% percentile, respectively, i.e., $\hat{D}^{(med)}(\zeta_{2,opt}, \beta_{opt})$, $\hat{D}^{(16)}(\zeta_{2,opt}, \beta_{opt})$, $\hat{D}^{(84)}(\zeta_{2,opt}, \beta_{opt})$. Coefficients $\bar{a}^{(\psi)}$ to $\bar{l}^{(\psi)}$ are fitted utilizing the same procedure as described for the corresponding coefficients of Eqs. (16) and (17), and they are listed in Appendix A and Tributsch and Adam (2012).

Median response coefficients for arbitrarily *detuned* TMD parameters ζ_2 and β are determined by multiplying the median coefficients for optimal TMD parameters $\zeta_{2,opt}$ and β_{opt}

$$\hat{R}^{(med)}(\zeta_2, \beta) = \gamma_R R^{(med)}(\zeta_{2,opt}, \beta_{opt}) \tag{19}$$

$$\hat{D}^{(med)}(\zeta_2, \beta) = \gamma_D D^{(med)}(\zeta_{2,opt}, \beta_{opt}) \tag{20}$$

at which

$$\gamma_R = 1 + \frac{n(\zeta_2 - \zeta_{2,opt})^2}{\zeta_2^o} + p(\zeta_2 - \zeta_{2,opt}) + [(|q| - |r|\zeta_2)|(\beta - \beta_{opt}) - s(\zeta_2 - \zeta_{2,opt})|^t]^2$$
$$+ u\zeta_1(\beta - \beta_{opt}) \tag{21}$$

$$\gamma_D = 1 + \bar{n}(1 + \bar{o}\zeta_2)((\beta - \beta_{opt})^2 + \bar{p}(\beta - \beta_{opt})) + \bar{q}(\beta - \beta_{opt})$$
$$\bar{r}|\zeta_2 - \zeta_{2,opt}|^{\bar{s}} + \bar{t}(\zeta_2 - \zeta_{2,opt}) \tag{22}$$

Coefficients n to u, and $\bar{n}$ to $\bar{t}$ in expressions (21) and (22) are not constant but depend itself on the mass ratio μ and inherent damping ζ_1. For details see again Tributsch and Adam (2012).

6.2 Validation

Subsequently, the approximation of the response quantities by analytical expressions is verified via the goodness-of-fit measure R^2 (Weisberg 2005). The maximum possible value of $R^2 = 1$ means that all the numerically derived values and the corresponding analytical values are identical. For a value of $R^2 = 0$ the actual approximation and the mean of all data is of the same quality. For values of $R^2 < 0$ the analytical expressions lead to an approximation worse than the mean. Additionally, the RMS of the relative error of the analytical approximations with respect to the simulated response quantities is determined.

Furthermore, simulations for a second set of far-field ground motions, denoted as LMSR-N, have been performed to confirm the findings of this study and to show the general applicability of the proposed analytical relations.

In Table 2 the derived goodness-of-fit measure R^2 and the RMS of the relative error, based on the entire parameter range, is specified for the response quantities $\hat{R}^{(med)}$, $\hat{P}^{(med)}$, and $\hat{D}^{(med)}$. They are provided for analytical approximations optimized for each ground motion set separately (columns 4, 5, 6 of Table 2), and optimized for all ground motion sets simultaneously (column 3 of Table 2).

It is readily observed that all R^2 values for the RMS displacement reduction coefficient $\hat{R}^{(med)}$ and for the TMD stroke coefficient $\hat{D}^{(med)}$ are close to one, and almost unaffected by the considered earthquake set. That means, for these response quantities global analytical relations can be provided. However, the peak displacement reduction coefficient $\hat{P}^{(med)}$ depends more pronounced on the considered set of ground motions, indicted by a smaller R^2 value for the simultaneous optimization

Table 2 Statistical validation of analytical relations

Coefficient		Analytical relations optimized for			
		ATC63-FF, ATC63-NFwP, LMSR-N	ATC63-FF	ATC63-NFwP	LMSR-N
$\hat{R}^{(med)}$	R^2	0.9639	0.9687	0.9728	0.9702
	Std.dev.	5.04%	4.67%	4.58%	4.33%
$\hat{P}^{(med)}$	R^2	0.7720	0.9122	0.8377	0.9010
	Std.dev.	5.48%	3.22%	3.84%	3.72%
$\hat{D}^{(med)}$	R^2	0.9816	0.9908	0.9894	0.9880
	Std.dev.	4.68%	3.24%	3.31%	4.06%

on three earthquake sets ($R^2 = 0.7720$) compared the outcomes for individual optimizations. It can be concluded that overall analytical relations can be used for the TMD assessment in an earthquake environment. However, the differentiation between near-fault and far-field earthquake excitation leads to a more precise assessment.

6.3 Application

In the following selected results of the TMD assessment according to the proposed analytical relations are depicted. These results are based on TMD parameter tuning according to Eqs. (13) and (15), and $\zeta_1 = 0.01$. Fig. 14 shows contour plots of the analytically derived RMS displacement reduction coefficients $\hat{R}^{(med)}$ (Fig. 14(a)), $\hat{R}^{(16)}$ (Fig. 14(b)), and $\hat{R}^{(84)}$ (Fig. 14(c)) for mass ratios μ between 0.5% and 8%, and periods T_1 ranging from 0.1 s to 5.0 s. Setting these outcomes in contrast with the corresponding plots for $R^{(med)}$ (Fig. 2(a)), $\hat{R}^{(16)}$ (Fig. 6(a)), and $\hat{R}^{(84)}$ (Fig. 6(b)) demonstrates that the analytical expression Eq. (16) approximates the actual counterparts with errors smaller than 10%. The same holds true for the median peak displacement reduction coefficient $\hat{P}^{(med)}$ and the stroke coefficient $\hat{D}^{(med)}$ depicted in Fig. 15, compare with Figs. 3(a) and 9(a).

Furthermore, in Figs. 16 and 17 cumulative distribution functions for the reduction coefficients R_i and P_i are presented for discrete pairs of periods T_1 and mass ratios μ. The results of these figures are examined in an effort to assess the analytical approximation of the response quantities. For each pair (T_1, μ) three different outcomes are presented. Sorting the individual outcomes based on the 44

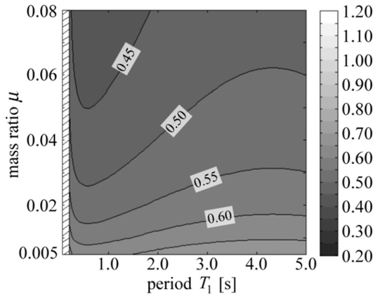

(a)

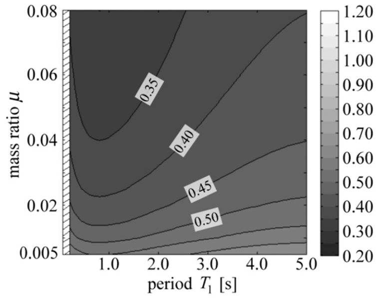

(b)

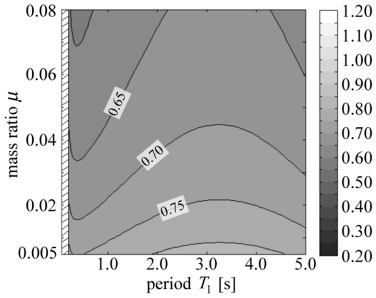

(c)

Fig. 14 RMS displacement reduction coefficient. Approximation. (a) Median, (b) 16% quantile and (c) 84% quantile. 0.20s ≤ T_1 ≤ 5.0s. $\zeta_1 = 0.01$. β_{opt} and $\zeta_{2,opt}$

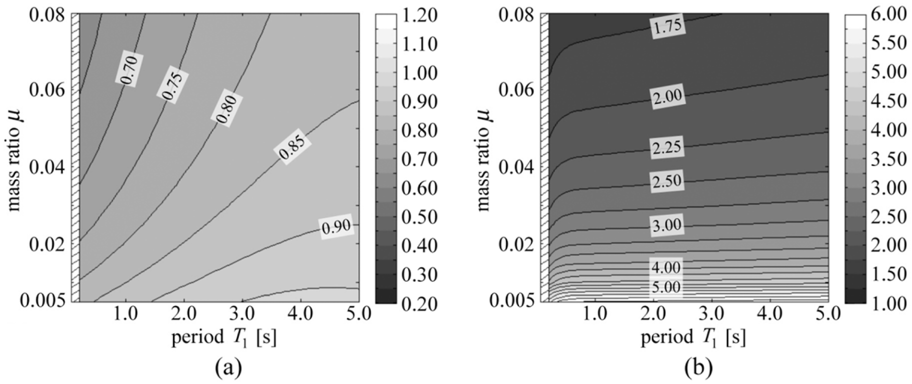

Fig. 15 (a) Peak displacement reduction coefficient based on the ATC63 far-field ground motion set and (b) TMD stroke coefficient. Approximation. Median. $\zeta_1 = 0.01$. β_{opt} and $\zeta_{2,opt}$

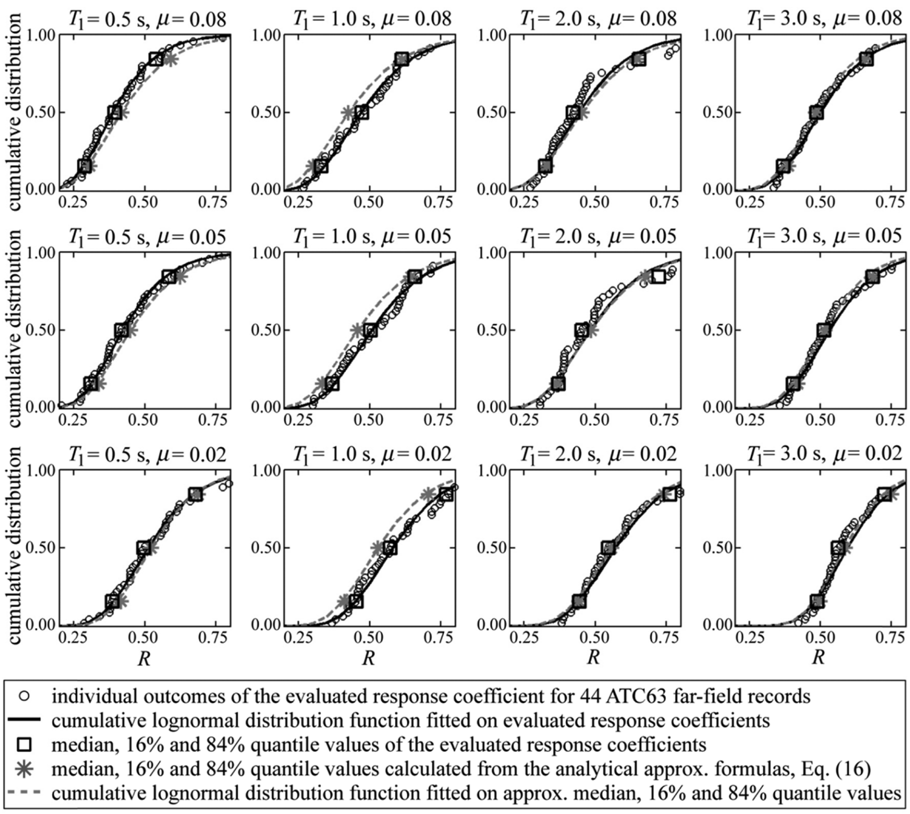

Fig. 16 Comparison of evaluated and approximated RMS displacement reduction coefficient. ATC63 far-field ground motion set. Discrete pairs of T_1 and μ. $\zeta_1 = 0.01$. β_{opt} and $\zeta_{2,opt}$

ground motions of ATC63-FF set yields the “exact” distribution marked with circles. The full line is the outcome of a lognormal approximation based on the individual outcomes. The dashed line refers also to the assumption of a lognormal distribution, however, median, 16% quantile and 84% quantile according to the analytical functions presented in Eq. (16) enter the analysis.

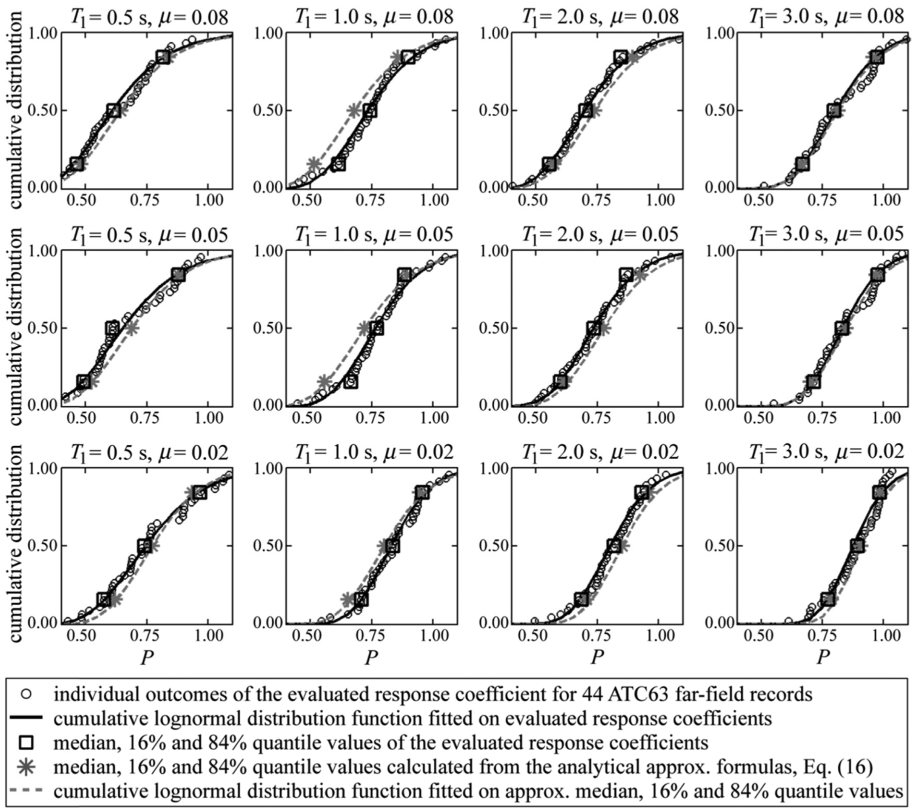

Fig. 17 Comparison of evaluated and approximated stroke coefficient. ATC63 far-field ground motion set. Discrete pairs of T_1 and μ. $\zeta_1 = 0.01$. β_{opt} and $\zeta_{2,opt}$

	A	B	C	D	E	F	G	H	I	J	K
1											
2	**Estimated coefficients *R*, *P* and *D***										
3											
4	**Input**										
5	Period [s]:	1,2	s	valid: 0,20 - 5,0							
6	damping coeff. ζ_1 [-]	0,010		valid: 0,005 - 0,05							
7	mass ratio μ [-]:	0,050		valid: 0,005 - 0,08							
8											
9	freq. ratio β_{opt} [-]	0,940									
10	damping coeff. $\zeta_{2,opt}$ [-]	0,110									
11											
12	freq. ratio β_{chosen} [-]	0,940		valid: 0,85 - 1,04							
13	damping coeff. $\zeta_{2,chosen}$ [-]	0,180		valid: 0,04 - 0,20							
14											
15	**Results**										
16	***R*** (RMS of structural displacement)			***P*** (peak struct. displ.)	ATC63FF	ATC63NFwP	LMSRN	3 sets		***D*** (TMD stroke)	
17	$R^{(16\%Q)}$	0,339		$P^{(16\%Q)}$	0,569	0,611	0,527	0,565		$D^{(16\%Q)}$	1,719
18	$R^{(med)}$	0,463		$P^{(med)}$	0,733	0,776	0,698	0,733		$D^{(med)}$	2,104
19	$R^{(84\%Q)}$	0,652		$P^{(84\%Q)}$	0,902	0,931	0,886	0,906		$D^{(84\%Q)}$	2,536
20											
21											
22	$R^{(med)}$ detuned	0,483								$D^{(med)}$ detuned	1,622
23		(+4,2%)									(-22,9%)

Fig. 18 Example of an analytical approximation of the proposed coefficients in a spreadsheet calculation

It is confirmed that a lognormal distribution describes very accurately the actual distribution of the individual outcomes of reduction coefficients, which is a result of the record-to-record variability. Moreover, the lognormal distribution based on analytical statistical values according to Eq. (16) leads to a sufficiently accurate approximation of the actual cumulative distribution. This observation supports the proposed analytical relations for assessing the seismic TMD performance.

Eqs. (16) to (22) have been implemented in an Excel sheet to provide an efficient tool for the fast assessment of the TMD performance. As an example, Fig. 18 shows a screenshot of this sheet. For the considered structure-TMD assembly (period, damping coefficient, mass ratio) with an assigned TMD damping coefficient of 18% (which is larger than the optimal value of 11%) the median RMS of displacement is reduced by about 54% ($R^{(med)} = 0.463$)). Detuning has only small effect on that value. The maximum displacement is reduced by about 27% ($P^{(med)} = 0.733$), and is also barely influenced by detuning. On the other hand, TMD damping of 18% decreases the stroke coefficient by more than 20% (compared to the outcome if a perfectly tuned TMD) to a value of about 1.62.

7. Conclusions

The results of a comprehensive parametric study have been presented, aiming at quantifying the seismic performance of Tuned Mass Dampers (TMDs). Vibration-prone structures are modeled as linear single-degree-of-freedom (SDOF) systems. An attached viscously damped SDOF oscillator serves as TMD. The study is based on several sets of recorded ground motions in order to capture the record-to-record variability of the response.

Tuning of the TMD parameters, i.e., the frequency ratio and its viscous damping ratio, has been assessed with the result that optimal tuning is possible for each single earthquake event. However, the mean of the individually optimized TMD parameters is in good agreement with the well-known analytical relations for white noise base excitation.

The effect of mass ratio, decoupled structural period, and inherent damping of the main structure on the TMD efficiency has been explored. In particular, the impact of a TMD on the structural displacement characterized by both its peak value and its RMS has been studied. The individual outcomes for each seismic record have been evaluated statistically for each set of ground motions.

Reviewing the results reveals that the seismic performance of the TMD is robust against detuning of viscous damping of the TMD. However, TMD damping larger than its optimal value reduces the stroke drastically without impairing the TMD efficiency considerably. This displacement reduction has been quantified, because in real systems the deflection of the mechanical spring element is limited. It has been shown that the impact of different ground motion sets is of minor significance.

The major findings of the study can be summarized as follows:

- Depending on the period and the mass ratio the TMD application leads to a median reduction of the RMS of the structural displacement between 40% and 55% for inherent structural damping of 1%, and 15% to 30% for inherent structural damping of 5%.
- The statistical evaluation shows that in 84% of all investigated seismic events the reduction of this response quantity is at least 15% for 1% inherent structural damping.
- The median peak displacement of the structure is reduced by 10% to 30% for 1% damped structures, and up to 15% for 5% damped structures, respectively.
- For structures with low inherent damping the TMD does not impair the structural performance in at least 84% of all investigated seismic events. Hence, there may be single seismic events, where

a TMD even leads to a slight amplification of the structural peak displacement.

- The reduction of the RMS of the structural displacement is almost independent from the considered earthquake set. However, during near-field earthquakes the structural peak displacement is not reduced as efficiently as during far-field excitations.
- The stroke is about 1.75 to 3.25 times the peak displacement of the unprotected structure, depending primarily on the mass ratio, however, almost unaffected by the inherent structural damping.
- Intentionally detuned TMD damping (of e.g., +5 percentage points) reduces the median stroke significantly (by about 17%) leaving the RMS and peak structural displacement almost unaffected (impaired by 1% to 2% only).

Based on the extensive database of results analytical design expressions for the discussed response quantities have been derived through non-linear regression analysis. It has been shown that these analytical relations are generally valid for earthquake excitation, because the goodness-of-fit measure R^2 is in general close to one. The median, 16% and 84% quantiles are specified to capture the record-to-record uncertainties under the assumption of a log-normal distribution. Thus, these relations allow the engineer in practice a fast and yet accurate assessment of the seismic TMD performance.

References

Adam, C. and Furtmüller, T. (2010), *Seismic performance of tuned mass dampers, Mechanics and model-based control of smart materials and structures*, (Eds., Irschik, H., Krommer, M., Watanabe, K. and Furukawa, T.), Springer, Wien, New York.

Ankireddi, S. and Yang, H.T.Y. (1996), "Control methodology for tall buildings subject to wind loads", *J. Struct. Eng. - ASCE*, **122**(1), 83-91.

Bachmann, H. and Weber, B. (1995), "Tuned vibration absorbers for 'Lively' structures", *J. Struct. Eng. - ASCE*, **5**(1), 31-36.

Casciati, F. and Giuliano, F. (2009), "Performance of multi-TMD in the towers of suspension bridges", *J. Vib. Control*, **15**(6), 821-847.

Chopra, A. (2006), *Dynamics of structures: theory and application to earthquake engineering*, 3rd Ed., Pearson Prentice Hall, NJ.

FEMA P-695 (2009), *Quantification of building seismic performance factors*, Federal Emergency Management Agency, Washington D.C.

Giuliano, F. (2012), "Note on the paper »Optimum parameters of tuned liquid column–gas damper for mitigation of seismic-induced vibrations of offshore jacket platforms« by Seyed Amin Mousavi, Khosrow Bargi, and Seyed Mehdi Zahrai", *Struct Health Monit*., DOI: 10.1002/stc.1499.

Hoang, N., Fujino, Y. and Warnitchai, P. (2005), "Design of multiple tuned mass dampers by using a numerical optimizer", *Earthq. Eng. Struct. D*., **34**(2), 124-144.

Hoang, N., Fujino, Y. and Warnitchai, P. (2008), "Optimal tuned mass damper for seismic application and practical design formulas", *Eng. Struct*., **30**(3), 707-715.

Jagadish, G.K. and Jangid, R.S. (2008), "Semi-active friction dampers for seismic control of structures", *Smart Struct. Syst*., **4**(4), 493-515.

Lee, C.L., Chen, Y.T., Chung, L.L. and Wang, Y.P. (2006), "Optimal design theories and applications of tuned mass dampers", *Eng. Struct*., **28**(1), 43-53.

McGill, R., Tukey, J.W. and Larsen, W.A. (1978), "Variations of Boxplots", *Am. Stat*., **32**(1), 12-16.

Marano, G.C., Greco, R. and Sgobba, S. (2010), "A comparison between different robust optimum design approaches: Application to tuned mass dampers", *Probabisist. Eng. Mech*., **25**(1), 108-118.

Marano, G.C., Greco, R., Trentadue, F. and Chiaia, B. (2007), "Constrained reliability-based optimization of linear tuned mass dampers for seismic control", *Int. J. Solids Struct*., **44**(22-23), 7370-7388.

Medina, R.A. and Krawinkler, H. (2003), *Seismic demands for nondeteriorating frame structures and their dependence on ground motions*, Report no. 144. The John A. Blume Earthquake Engineering Center, Stanford University.

Meinhardt, C. (2010), “Experimental damping assessments of tall buildings to verify the effectivity of damping devices for high rise structures”, *Proceedings of the Highrise Towers and Tall Buildings 2010*, Munich, Germany.

Rüdinger, F. (2006), “Optimal vibration absorber with nonlinear viscous power law damping and white noise excitation”, *J. Eng. Mech. - ASCE*, **132**(1), 46-53.

Schmelzer, B., Oberguggenberger, M. and Adam C. (2010), “Efficiency of tuned mass dampers with uncertain parameters on the performance of structures under stochastic excitation”, *J. Risk Reliab*., **224**(4), 297-308.

Tributsch, A. and Adam, C. (2012), *Application of tuned mass dampers in an earthquake environment*, Internal report, University of Innsbruck, Austria.

Tributsch, A., Adam, C. and Furtmüller, T. (2011), “Mitigation of earthquake induced vibrations by tuned mass dampers”, *Proceedings of the EURODYN 2011*, Leuven, Belgium.

Wang, J.F., Lin, C.C. and Lian, C.H. (2009), “Two-stage optimum design of tuned mass dampers with consideration of stroke”, *Struct. Health Monit*., **16**(1), 55-72.

Warburton, G.B. (1982), “Optimum absorber parameters for various combinations of response and excitation parameters”, *Earthq. Eng. Struct. D*., **10**(3), 381-401.

Weisberg, S. (2005), *Applied linear regression*, 3rd Ed., Wiley.

Woo, S.S., Lee, S.H. and Lan, C. (2011), “Seismic response control of elastic and inelastic structures by using passive and semi-active tuned mass dampers”, *Smart Struct. Syst*., **8**(3), 239-252.

FC

Appendix A

Table 3 Coefficients, which enter the analytical response relations, compare with Eqs. (16) to (18)

	ATC63-FF, ATC63-NFwP, LMSR-N				ATC63-FF				ATC63-FF, ATC63-NFwP, LMSR-N		
	$R^{(16)}$	$R^{(med)}$	$R^{(84)}$		$P^{(16)}$	$P^{(med)}$	$P^{(84)}$		$D^{(16)}$	$D^{(med)}$	$D^{(84)}$
a	0,1610	0,1834	0,1554	$\tilde{a}$	0,5514	0,4727	-0,0279	$\bar{a}$	0,0618	0,0586	0,0069
b	0,07743	0,01005	0,00356	$\tilde{b}$	0,3540	0,4254	0,2300	$\bar{b}$	0,1903	-0,0473	-0,1247
c	0,2944	-0,0822	-0,1180	$\tilde{c}$	2,6076	2,5820	6,4249	$\bar{c}$	-3,2493	-2,3117	-0,9988
d	-0,6497	-0,8365	-0,7105	$\tilde{d}$	0,0128	0,0193	0,3112	$\bar{d}$	-4,6288	-3,3702	-3,0120
e	-0,1678	-0,1445	-0,2485	$\tilde{e}$	0,0289	0,0447	0,1918	$\bar{e}$	0,0445	0,0505	0,0507
f	-1,4971	-4,2561	-0,9759	$\tilde{f}$	-153,62	-53,549	-10,3341	$\bar{f}$	0,0377	0,0206	0,0129
g	-31,345	-25,384	-1,9858	$\tilde{g}$	-8,7675	-3,2429	-0,5172	$\bar{g}$	0,3603	0,2750	0,2093
h	0,00436	0,00494	0,01102	$\tilde{h}$	0,0390	0,0783	0,1894	$\bar{h}$	6,8936	6,7394	15,604
i	0,0110	0,0153	0,0394	$\tilde{i}$	0,8839	1,2783	-26,7799	$\bar{i}$	-0,3330	-0,6430	0,8883
j	0,0547	0,0534	0,0550	$\tilde{j}$	0,5896	0,7140	2,3450	$\bar{j}$	3,6306	2,9156	1,7779
k	3,6874	2,1893	2,1767					$\bar{k}$	0,3107	0,3467	0,2893
l	0,5165	0,2977	0,2888					$\bar{l}$	0,2572	0,7376	1,3058
m	-0,1769	-0,1118	-0,1036								